International Journal of Thermophysics, Vol. 24, No. 1, January 2003 (© 2003)

Influence of Thermal Properties on the Sensitivity of Thermal Wave Interferometry for the Characterization of Plasma-Sprayed Coatings

A. Bendada,[1,2] M. Lamontagne,[1] and H. Roberge[1]

Received June 18, 2002

Thermal wave interferometry (TWI) is used as a means for measuring the thermal properties of plasma-sprayed coatings. The solution of the inverse problem is influenced by the magnitude of the signal-to-noise ratio and the amount of data available. This is investigated using a sensitivity analysis. The critical factors that determine the accuracy and the limitations of the technique are discussed. Numerical and experimental thermal wave tests confirm the range of applicability and the accuracy of TWI for measuring thermal properties.

KEY WORDS: coatings; effusivity; plasma-spray; sensitivity analysis; thermal conductivity; thermal diffusivity; thermal waves; zirconia.

1. INTRODUCTION

Thermal barrier coatings (TBCs) are increasingly used to protect the base metal and allow higher operating temperatures in gas turbine and diesel engine components. Plasma-sprayed stabilized zirconia coatings can reduce the heat flow and thus the cooling requirements by up to 80%, depending on the thickness and the thermal conductivity of the coating material. It is necessary to non-destructively evaluate their thermal properties in order to know their effectiveness as thermal barriers. In-service inspection is particularly attractive to analyze the change of the coating thermal properties which may be affected by irreversible thermal conductivity or hot-corrosion of the coating.

[1] National Research Council, Industrial Materials Institute, 75 De Mortagne Boulevard, Boucherville, QC, J4B 6Y4, Canada.
[2] To whom correspondence should be addressed. E-mail: abdelhakim.bendada@nrc.ca

0195-928X/03/0100-0207/0 © 2003 Plenum Publishing Corporation

There have been a number of non-destructive methods used to determine the thermal propeties of TBCs. The majority of these methods rely on laser-modulated or pulsed-heating techniques [1–15]. They are valuable because they are single-sided and non-contacting. Modulated techniques have been shown to be potentially appropriate for the characterization of thermally sprayed coatings. They can be used for the quantitative evaluation of the coating thickness or thermal properties, and to image adhesion defects at the interface as well [1, 4, 6, 9].

The present paper, which deals with thermal wave interferometry, discusses the effect of the thermal characteristics on the sensitivity of the method. A sensitivity study was carried out analytically for various values of the thermal properties, and the factors influencing the effectiveness of the method were established. To validate these factors, a first simulation using noisy data generated numerically was performed. The technique was then applied to the characterization of three samples of yttrium-stabilized zirconia (YSZ) plasma-sprayed onto copper. The results were compared to measurements provided by the laser flash method [8, 10, 12] and modulated differential scanning calorimetry. Discrepancies are discussed in terms of coating thickness and sensitivity of TWI in determining the thermal parameters.

2. DESCRIPTION OF THE TWI TECHNIQUE

2.1. Theory

In the TWI technique, the coating surface is heated periodically and the resulting periodic thermal response, governed by the heat diffusion equation, is monitored. The basic principle of TWI is that, when thermal waves are generated in a coating-substrate sample, they propagate diffusively to the interface, where they are partially reflected and return to produce interference effects at the surface. The interference between the reflected and the incoming thermal waves leads to variations in the surface temperature. According to theoretical modeling [1, 3], the changes in the surface temperature T caused by TWI for an opaque homogeneous coating material of thickness L are given by

$$T = \frac{Q_0}{2k_c\sigma}\frac{1+R\exp(-2\sigma L)}{1-R\exp(-2\sigma L)} \tag{1}$$

in which Q_0 is the incident radiant flux, k_c and σ are the thermal conductivity and complex thermal wavenumber defined as $\sigma = (1+j)/\mu$, where μ is the thermal diffusion length $\mu = (\alpha_c/\pi f)^{1/2}$, α_c is the normal thermal

diffusivity, f is the frequency; R is the thermal wave reflection coefficient defined as $R=(1-b)/(1+b)$, and $b=[(\rho C_p k)_s/(\rho C_p k)_c]^{1/2}$ gives the ratio of the substrate and coating thermal effusivities e_s and e_c.

In Eq. (1), the temperature at the surface is a complex quantity, which is physically interpreted as arising from the fact that the temperature at the surface is out of phase with the heating source. In practice, the experimental surface temperature is normalized by the surface temperature, obtained at the same conditions, of a semi-infinite homogeneous material (reference). The normalizing procedure is necessary to remove system frequency dependences from the experimental data. The normalized phase shift with respect to the applied periodic heating can be derived from the comparison of Eq. (1) and the theoretical expression of the surface temperature of a semi-infinite homogeneous solid [1, 2]; the phase signal is given by

$$\varphi=-\tan^{-1}\left[\frac{2R\exp(-x)\sin(x)}{1-R^2\exp(-2x)}\right] \tag{2}$$

in which $x=2L/\mu=2(\pi t_c f)^{1/2}$, where $t_c=L^2/\alpha_c$ represents the characteristic thermal diffusion time of the coating.

Typical interferometric patterns of the normalized phase change φ, against the reduced coating thickness L/μ are shown in Fig. 1 for a range of the coating/substrate reflection coefficients. A negative value of R

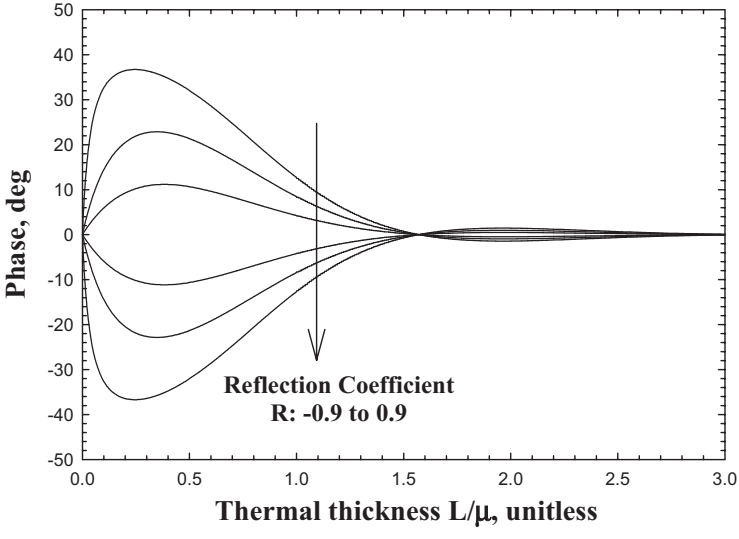

Fig. 1. Phase angle variation with coating thermal thickness for various coating/substrate reflection coefficients ($R=\pm 0.90, 0.60, 0.30$).

indicates a phase lead, and a positive value indicates a phase lag. The greater the magnitude of R, the larger is the phase change. Maximum interference effects occur when the coating thickness is less than a thermal diffusion length because of the heavily damped nature of thermal waves. It is usually possible to drive the thermal thickness into the interference region by choosing a suitable modulation frequency and coating thickness.

It can be clearly seen from Eq. (2) that the governing thermal quantities for the phase shift changes with frequency are the reflection coefficient R, and the characteristic thermal diffusion time t_c. The effusivity is involved in the phase signal through the reflection coefficient R, and the diffusivity through the characteristic thermal diffusion time t_c. A nonlinear least squares fitting of phase versus frequency measurements can then be used to identify the characteristic time t_c and the reflection coefficient R. The coating thermal diffusivity is obtained from the characteristic time if the coating thickness is known, and the coating thermal effusivity is obtained from the reflection coefficient if the substrate effusivity is known. It should be pointed out here that, even if the effusivity is the relevant parameter for time-dependent surface heating processes, the fact that it is estimated, through the reflection coefficient at the coating/substrate boundary, means that the information about effusivity is expected to be obtained from low modulation frequency scans. Indeed, because the thermal diffusion length μ varies as $(1/f)^{1/2}$, information about the thermophysical properties just at the surface is obtained for high frequencies, and subsurface information from deeper below the illuminated surface is obtained for low modulation frequencies.

In order to check the uniqueness and the reliability of the solution of the inverse problem, some issues have to be considered. One of them is the influence of the measurement noise on the unknowns. Another is the amount of experimental data available: insufficient data lead to error in the solution while too much data may give rise to correlation between parameters. This is analyzed using a sensitivity study of the normalized phase signal.

2.2. Sensitivity Analysis

The sensitivity analysis is carried out for a two-layer opaque homogeneous model. Structural properties affecting the thermal transport such as roughness and porosity, which may be met in plasma sprayed coatings, are not considered. The study is devoted to plasma-sprayed samples that have perfect adhesion at the coating-substrate interface, and very low level of roughness or polished surfaces so that roughness effects can be neglected. With very low-level roughness, the surface effects are strongest at higher

frequencies whereas the low frequencies are mostly related to the intrinsic coating and substrate properties. The analysis is also valid for rough surfaces after elimination of roughness effects from the phase frequency scans using mathematical methods [15].

The sensitivity coefficient is defined as the first derivative of a dependent variable, such as phase, with respect to an unknown parameter, such as thermal diffusivity [16–18]. Sensitivity to diffusivity and effusivity coefficients can easily be calculated through analytical derivation of Eq. (2). These coefficients depend on the units chosen for the parameter and also on its absolute value. To make the sensitivity analysis independent of units and absolute value (the unit system is arbitrary and the parameter absolute value is generally unknown), it is usually preferable to use the reduced sensitivity coefficients given by

$$S_{\alpha_c} = \alpha_c \frac{\partial \varphi}{\partial \alpha_c} = xR \frac{\exp(-x)[\cos(x) - \sin(x)] - R^2 \exp(-3x)[\cos(x) + \sin(x)]}{[1 - R^2 \exp(-2x)]^2 + 4R^2 \exp(-2x) \sin^2(x)} \tag{3}$$

$$S_{e_c} = e_c \frac{\partial \varphi}{\partial e_c} = \frac{(R^2 - 1) \exp(-x)[1 + R^2 \exp(-2x)] \sin(x)}{[1 - R^2 \exp(-2x)]^2 + 4R^2 \exp(-2x) \sin^2(x)} \tag{4}$$

These coefficients can show areas of difficulty and lead to improvements in the experimental design. Beck and Arnold [16] have shown that if the sensitivity coefficients are small or correlated with one another within the interval of the independent variable (in this case, frequency) used for their identification, the inverse problem is difficult and very sensitive to measurement noise and errors (small errors in the data can cause a large variation in the solution).

The notion of correlation (or linear dependence) can be studied if each sensitivity coefficient is considered as a function of the independent variable [16, 17]. Figure 2 shows a typical plot of the two sensitivity functions S_{α_c} and S_{e_c}, together with the phase φ plotted versus the thermal thickness L/μ for a reflection coefficient $R = -0.30$ (in other words, for a specific value of the effusivity e_c). The effect of the diffusivity α_c is implicitly taken into account in the unitless abscissa L/μ. The use of the thermal thickness L/μ as an abscissa is very practical since it reduces the number of variables in the mathematical model and allows a global presentation of the effects of the diffusivity α_c, the coating thickness L, and the frequency f on the sensitivities and the phase. For the sake of clarity, only negative R values were considered; positive R values affect only the sign of the phase and the reduced sensitivity to the diffusivity functions [Eqs. (2)–(4)]. Therefore, all the results given in this paper are also valid for positive R values. The

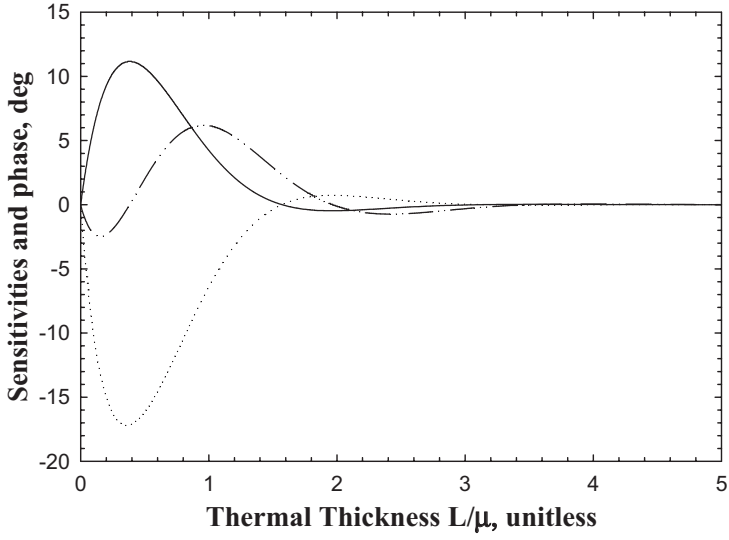

Fig. 2. Phase angle and its sensitivities to thermal diffusivity and effusivity versus coating thermal thickness for a reflection coefficient $R = -0.30$ (Solid line: Phase; Dashed line: S_{α_c}; Dotted line: S_{e_c}).

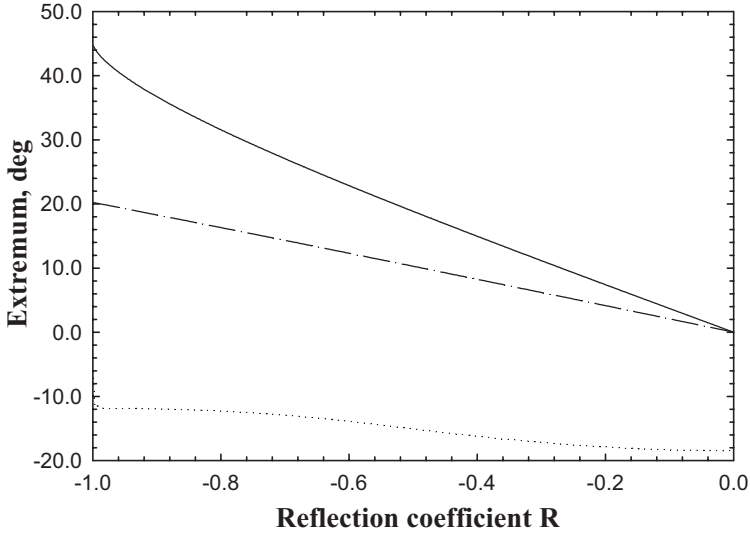

Fig. 3. Variation of the extremum values of phase angle and sensitivities to thermal diffusivity and effusivity with reflection coefficient (Solid line: Extremum of phase; Dashed line: Extremum of S_{α_c}; Dotted line: Extremum of S_{e_c}).

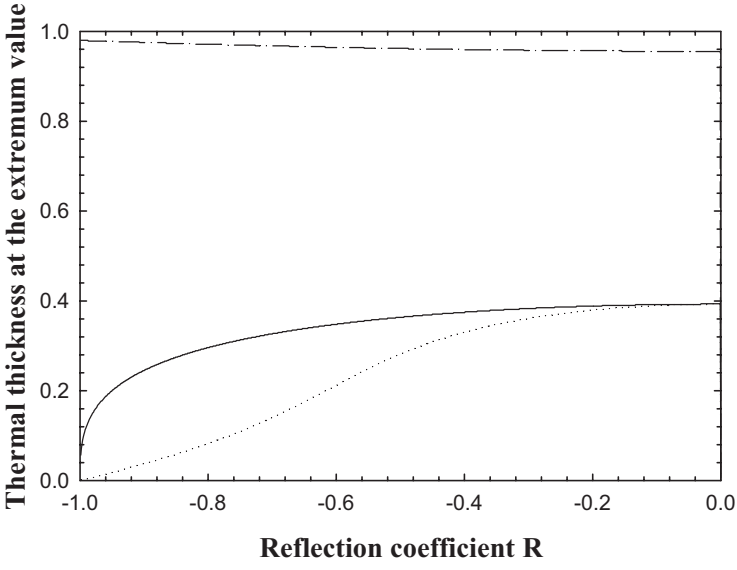

Fig. 4. Variation of thermal thickness at the extremes of phase angle and sensitivities to thermal diffusivity and effusivity with reflection coefficient (Solid line: L/μ of phase extremum value; Dashed line: L/μ of S_{α_c} extremum value; Dotted line: L/μ of S_{e_c} extremum value).

coordinates of the extremum values of φ, S_{e_c}, and S_{α_c} were extracted from curves similar to those plotted in Fig. 2, and obtained for various values of the reflection coefficient R. The extremum coordinates are plotted versus R in Figs. 3 and 4. The following points deserve to be emphasized:

- The extremum values of S_{e_c} appear for thinner thermal thicknesses than those of S_{α_c} (Fig. 4), which means that simultaneous identification of both e_c and α_c is theoretically possible (independence of the sensitivity coefficients) [16].
- Since the extremum values of S_{e_c} appear for thinner thermal thicknesses than those of S_{α_c} (Fig. 4), particularly for R in the range -1 to -0.5, accurate effusivity estimation will be very difficult for cases where phase data are limited to larger thermal thicknesses. This may happen, for example, for certain experimental designs limited to low frequencies when characterizing thermally thick coatings.
- The maximum sensitivity to α_c and the phase angle φ increase almost linearly with the absolute value of R (Fig. 3). This means that larger absolute values of R lead to more precise estimations of α_c.

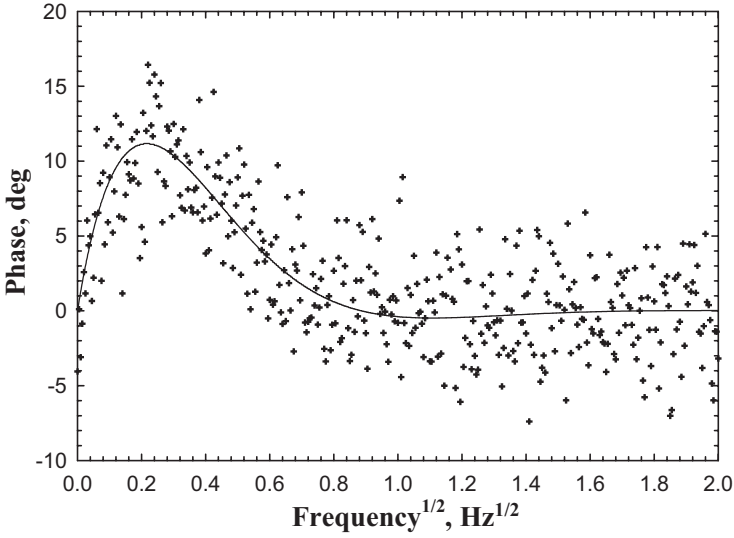

Fig. 5. Noisy phase signal generated numerically for a reflection coefficient $R = -0.30$ and a random normal noise of zero mean and a standard variation of 4 deg.

- The maximum sensitivity to e_c decreases slightly when R varies from 0 to -1 (Fig. 5), except when R becomes very close to -1, where S_{e_c} suddenly drops to zero. In other words, the precision of the estimated effusivity is not very dependent on the absolute value of R, except for $R \cong -1$ where $S_{e_c} \cong 0$ (Fig. 3).
- The extremum value of S_{e_c} is larger than that of S_{α_c} for $|R| < 0.65$, and S_{α_c} tends to zero when R tends to zero. For those small values, the maximum sensitivity to e_c is located near the maximum phase angle (Fig. 2). On the other hand, the extremum value of S_{e_c} is slightly lower than S_{e_c} for large values of R; therefore, it is easier to better identify α_c than e_c when R is large.
- The extremum value of the sensitivity to the diffusivity occurs in the decreasing region of the phase signal. Specifically, it occurs at the inflexion point of the decreasing part of the phase, at a thermal thickness close to 1. This is applicable for any value of the reflection coefficient R as is clearly shown by Fig. 4. The best one-point identification procedure of α_c is obtained using the inflection point of the decreasing part of the phase signal. As an approximation, this point is located near the half maximum of the phase signal.

– The sensitivity to α_c cancels out (exact zero value) when the thermal thickness corresponds to the maximum of the phase curve (Fig. 2). This means that an estimation using data in the maximum phase region, and particularly a maximum point identification procedure, are not suitable for effective identification of the diffusivity.

2.3. Numerical Simulation

To illustrate the sensitivity analysis, Eq. (1) was first used to generate an exact phase signal for a reflection coefficient $R = -0.30$ and a characteristic time $t_c = L^2/\alpha_c = 1$ s. To assess the effect of noisy data on the identified parameters (R and t_c), a normal noise with zero mean and a standard deviation of 4 degrees was added to the exact data. Both exact and noisy data are plotted in Fig. 5.

Curve fittings were carried out using Simplex least-squares routine. Two fits were performed. The first one used only data in the region of maximum sensitivity to the effusivity (in this case, region of the maximum phase signal), while the second one used only data in the region of maximum sensitivity to the diffusivity (region of the half maximum point in the decreasing part of the phase signal). The initial parameters for both minimizations were $R^{(0)} = -0.9$ and $t_c^{(0)} = 0.1$ s.

The first fitting gave the following estimations: $R = -0.297$ and $t_c = 0.590$ s, and the errors were $\Delta R/R = -1\%$ and $\Delta t_c/t_c = -41\%$, respectively. Using the relationships $e_c = e_s(1+R)/(1-R)$ and $\alpha_c = L^2/t_c$, it was also possible to evaluate the corresponding errors on the effusivity and the diffusivity. As expected from the sensitivity study, the error for e_c ($\Delta e_c/e_c = +0.065\%$) was lower than the one for α_c ($\Delta\alpha_c/\alpha_c = +41\%$).

The second simulation gave $R = -0.412$ and $t_c = 1.241$ s, and the errors were $\Delta R/R = 40\%$ and $\Delta t_c/t_c = 24\%$. The corresponding errors for the effusivity and the diffusivity were $\Delta e_c/e_c = -26\%$ and $\Delta\alpha_c/\alpha_c = -24\%$. This time, the errors were similar for both parameters. This was expected since the sensitivities to both parameters are of the same magnitude in this region (Fig. 2). The results were inaccurate for both parameters because of the low sensitivity magnitudes for $R = -0.30$ (Fig. 3) and the low signal-to-noise ratio (Fig. 5).

3. DESCRIPTION OF THE EXPERIMENTAL SETUPS

3.1. Thermal Wave Interferometry

Thermal waves were generated by a modulated diode laser beam (Opto Power OPC-B015-FCTS), which was adjusted to provide an optical

power of 2.75 W. The energy emission wavelength was 830 nm, and the heating beam was modulated by the control unit of the diode laser at frequencies in the range of 0.5 to 100 Hz.

The determination of the thermal properties of a coating is only valid if the experimental conditions employed to obtain the data match the theoretical conditions assumed in the analysis of Bennett and Patty [3]. In this analysis, heat diffusion into the coating was taken to be one-dimensional. When heating the surface with a laser beam, this condition may be achieved provided that the diameter of the beam is much greater (by a factor exceeding seven) than the thermal diffusion length. This was ensured in the measurements at lower modulation frequency by expanding the diode laser beam spot size to a diameter larger than the test piece diameter. The use of an extended area of heating source also rendered negligible any effect that might be caused by lateral heat diffusion in the coating material. The uniformity of the surface temperature distribution was checked and confirmed using an AGEMA 900 long wave infrared camera.

The infrared emissions from the heated spot on the sample were monitored by a photovoltaic INSB detector (Optikon Corporation Ltd.), highly sensitive between 2 and 5.5 μm wavelength. A Germanium window with a transmission bandwidth of 2 to 14 μm was mounted in front of the detector to block any reflected radiation from the pump diode laser. The signal from the infrared detector was then processed by a lock-in amplifier (Stanford Research Systems SR530), which monitored both the amplitude and the phase of the input signal. The diode laser beam was taken as a reference signal, and its variation was provided by a high speed silicon detector, sensitive in the spectral range 400 to 1100 nm (Thorlabs PDA55).

As the zirconia coating is transparent, particularly in the infrared detector band and at the diode laser wavelength, a thin (1 μm thick) gold-palladium coating was sputtered on its surface to raise its opaqueness. For reference, we point out here that even for a translucent coating, the thermal properties can still be estimated but with a more complicated analysis [1, 6, 7, 11, 13, 14].

The measured signals were calibrated by using signals obtained under equal conditions for a homogeneous thick alumina specimen to remove instrumental phase shift.

3.2. Flash Method

The flash method was used to validate the diffusivity measured by the TWI tests because it is considered to be a reliable and accurate technique. The precision of the flash method is usually better than 5%. Since this technique requires access to both sides of the specimen, coatings were

separated from their substrates (Section 4). A YAG laser pulse of nearly 600 μs duration and 10 J energy was projected over the full 15 mm diameter face of the sample. The back temperature evolution was monitored by the same infrared detector as used in the TWI experiments.

Once again, because zirconia is transparent, it was necessary to add thin gold-palladium coatings (1 μm thick) to both faces of the samples. This prevented laser beam penetration and the detector from viewing the bulk.

3.3. Differential Scanning Calorimetry

Heat capacity measurements were carried out using a Q1000 Modulated Differential Scanning Calorimeter (MDSC) of TA Instruments to check the validity of the effusivity obtained in the TWI operation. In MDSC, a sinusoidal modulation is overlaid onto a linear heating ramp to yield a heating profile in which the average sample temperature increases with time but not in a linear fashion. The selected measurement variables for the linear and oscillating components of this complex heating were as follows: Underlying heating rate: $2\,°C \cdot min^{-1}$; period of modulation: 60 s; temperature amplitude of operation: 0.318 °C. The Q1000 MDSC provides measurements precise to around 1%.

Knowing the heat capacity and the diffusivity measured by the flash method (Section 3.2), it was possible to evaluate the effusivity of the coating using the following relationship: $e_c = (\rho C_p)_c\,(\alpha_c)^{1/2}$. The bulk density ρ_c was calculated from sample geometry and mass. The precision of the effusivity estimated from both the flash method and the MDSC can thus be calculated from the previous expression. It was found to be around 1.5%.

4. DESCRIPTION OF THE SAMPLES

Three samples were produced by plasma-spraying, in air, the coating onto a copper substrate (copper thickness, 3 mm; previously sandblasted with 24-grit alumina under a pressure of 30 psi).

The plasma-spraying torch was a Plasmadyne SG100, with a No. 129 cathode and a No. 145 anode, ejection gas No. 113. The power was 33.3 kW (900 A and 37 V). The arc gas was argon, and the auxiliary gas was helium (32% helium, with $50\,\ell \cdot min^{-1}$ for argon and $23.6\,\ell \cdot min^{-1}$ for helium). The standoff distance during projection, over a surface of $120 \times 160\,mm^2$, was 76 mm. Spraying was carried out through circular masks (15 mm diameter) to better shape the sprayed area. The substrate

was cooled with a nitrogen jet, while the front surface was air-blasted to eliminate aerosols.

The three zirconia coatings (of 252, 317, and 500 μm thickness) were obtained with zirconia-8% yttria powder of granulometry 22.5 to 45 μm; Amperit, 825.1; powder flow, 22 $g \cdot min^{-1}$; and powder-carrying argon gas flow, 6.6 $\ell \cdot min^{-1}$. The torch was laterally scanned at 0.5 $m \cdot s^{-1}$.

To validate the thermal properties by the flash method and calorimetry, access to both sides of the coating was needed. Thus, after carrying out the interferometry tests, the coatings were separated from the substrates by chemical etching for 2 h in a 50% water solution of nitric acid, which did not substantially attack zirconia. The thickness fluctuations over the disk-shaped samples were of the order of the surface roughness, 10 μm.

5. RESULTS AND DISCUSSION

To test the reliability of the measurements obtained using thermal wave interferometry, and to illustrate the results of the sensitivity analysis, we compared the TWI diffusivity to the diffusivity measured by the flash method, and the TWI effusivity to the effusivity measured by combining the results of the MDSC and the flash method (Section 3.3). The flash and MDSC techniques are considered very reliable and highly accurate and can thus be used as reference techniques for the validation of TWI.

Measurements with the flash and MDSC experiments were performed after TWI measurements had been finished and the coatings had been separated from their substrates (Section 4). Diffusivity results obtained by the flash method are shown in Table I. Effusivity values estimated by combining the heat capacity measured by the MDSC technique and the diffusivity measured by the flash method (Section 3.3) are shown in Table II.

Substrate effusivity, which was needed, in the TWI technique, to extract the coating effusivity from the reflection coefficient, was determined by combining the flash method and the MDSC measurements: $e_s = 35899$ $J \cdot m^{-2} \cdot °C^{-1} \cdot s^{-1/2}$.

Table I. Coatings Diffusivity Obtained by the Flash Method

Sample No.	L (μm)	α_c (10^{-7} $m^2 \cdot s^{-1}$)
1	252	5.90
2	317	6.02
3	494	5.85

Table II. Coatings Effusivity Obtained by the Combination of the Diffusivity Measured by the Flash Method and the Heat Capacity Measured by the MDSC

Sample No.	L (μm)	ρ_c ($kg \cdot m^{-3}$)	$(C_p)_c$ ($J \cdot kg^{-1} \cdot °C^{-1}$)	e_c ($J \cdot m^{-2} \cdot °C^{-1} \cdot s^{-1/2}$)
1	252	4065	452	1411
2	317	4402	552	1885
3	494	4812	453	1667

The specimens under investigation were coatings of low thermal conductivity (zirconia) on a substrate of high thermal conductivity (copper); as a consequence, the reflection coefficient R was expected to be around -0.90. As previously discussed in the sensitivity analysis for large R values, this case is very suitable for good diffusivity estimation since S_{α_c} and φ are large. The effusivity should also be well estimated because it still has quite a high sensitivity at thin thermal thicknesses. However, since the coatings under investigation were thermally thick (large t_c), and because the experimental design was limited to frequencies larger than 0.5 Hz, the measurement was restricted to the decreasing part of the phase signal as shown in Fig. 6. This figure shows the fitting of experimental data for Sample 1

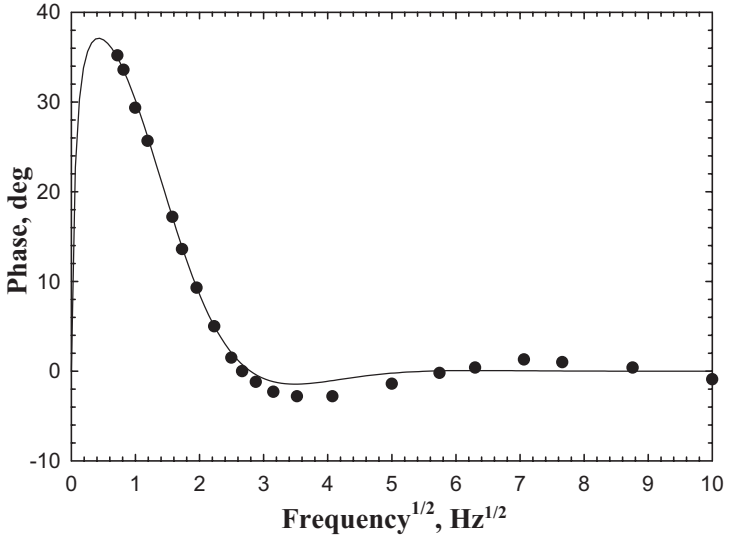

Fig. 6. Numerical fitting of the thermal diffusivity and effusivity for the thinner YSZ/copper coating (Sample 1, Thickness $L = 252$ μm).

($L = 252\ \mu m$). Sample 2 ($L = 317\ mm$) and Sample 3 ($L = 494\ \mu m$) are thicker than Sample 1. Consequently, for samples 2 and 3, the thermal thickness L/μ was restricted to high values. According to the sensitivity analysis for high R values, we did not expect to obtain precise estimations of e_c for these two samples. The reason is that, for high R values, the sensitivity to the effusivity reaches an extremum at very low thermal thicknesses (Fig. 4), and then changes rapidly to weak values at larger thermal thicknesses. However, diffusivity measurements were expected to be quite accurate. Indeed, the maximum sensitivity to diffusivity is within the large thermal thickness region (Fig. 4), and the lack of data at low frequencies did not have a serious effect on its estimation.

Table III summarizes the results obtained from all the samples analyzed by the TWI technique. We mention for reference that because of the low level of the roughness compared to the coating thickness, effects of roughness were neglected in the frequency range (0.5 to 100 Hz) used during the processing of the phase data. This assumption is based on the fact that for low roughness levels, the phase signal is affected by roughness only at high frequencies and less influenced at low frequencies where it exhibits the behavior of a homogeneous coating. This was confirmed experimentally by high frequency scans of the coatings; roughness effects manifested themselves, only starting from 3 kHz, by deviating the phase signal from the flat behavior of a normalized homogeneous sample.

It can be seen from Tables I and III that TWI provides diffusivity values comparable to those obtained with the flash method. However, the agreement was not as good for the effusivity, particularly for the thicker sample No. 3 (Tables II and III). Effusivity evaluations of thermally thick coatings are more dependent on coating thickness than diffusivity evaluations when the experimental design is limited to high frequencies (here, $f > 0.5$ Hz). Moreover, according to the sensitivity study, the errors in the effusivity due to frequency scan limitations are expected to increase for larger values of the reflection coefficient ($e_s \gg e_c$).

Table IV summarizes the discrepancies between the thermal properties provided by the TWI technique and those given by the flash and MDSC

Table III. Coatings Diffusivity and Effusivity Obtained by Thermal Wave Interferometry

Sample No.	L (μm)	α_c ($10^{-7}\ m^2 \cdot s^{-1}$)	R	e_c ($J \cdot m^{-2} \cdot °C^{-1} \cdot s^{-1/2}$)
1	252	6.31	−0.907	1754
2	317	6.21	−0.914	1615
3	494	5.62	−0.974	474

Table IV. Discrepancies of TWI with Respect to the Flash and the MDSC Measurements

Sample No.	L (μm)	$\Delta\alpha_c/\alpha_c$ (%)	$\Delta e_c/e_c$ (%)
1	252	+6.95	+24.31
2	317	+3.16	−14.32
3	494	−3.93	−71.57

measurements. It can be seen clearly that the identification of the diffusivity by TWI is quite acceptable. The diffusivity errors were less than 7%, which is comparable to the standard precision of the flash method, 5%. On the other hand, the absolute effusivity error was in the range 14 to 71%. These percentage errors are not comparable to standard effusivity evaluation techniques (accuracy $< 5\%$) and are too high to be acceptable. However, these errors must not necessarily eliminate TWI as a technique for evaluating the effusivity; effusivity, in this work, was obtained for unfavorable evaluation conditions: very high reflection coefficients (Table III) and large coating thicknesses. With the same experimental design, TWI should produce higher accuracy for the effusivity when the reflection coefficient and the coating thickness are low.

6. CONCLUSION

A sensitivity analysis has been performed to determine the critical parameters influencing the accuracy of the TWI technique for the evaluation of the thermal properties of TBCs. It was found that the technique yields reliable thermal diffusivity values for larger values of the reflection coefficient R. A large R coefficient arises for a coating of low thermal effusivity on a substrate of high thermal effusivity. On the other hand, the best effusivity measurements are obtained when R is low. However, if we consider the fact that the sensitivity of TWI to thermal effusivity does not depend much on R, and the phase signal is high at large R values, it can be stated that when R is high, both diffusivity and effusivity can be estimated with quite high accuracy.

Another important point must be taken into account: when the apparatus design does not allow measurements at low enough frequencies, such as for thermally thick coatings (large characteristic time $t_c = L^2/\alpha_c$), accurate effusivity measurements are very difficult to make, but diffusivity can still be accurately determined. That is because TWI is very sensitive to effusivity at thin thermal thicknesses (L/μ), and to diffusivity in the high

thermal thickness region. This was confirmed by characterizing three different thickness (different characteristic time) coatings of yttrium-stabilized zirconia (YSZ) plasma-sprayed onto a copper substrate.

REFERENCES

1. D. Almond and P. Patel, *Photothermal Science and Techniques* (Chapman & Hall, London, 1996).
2. J. A. Garcia, A. Mandelis, B. Farajbakhsh, C. Lebowitz, and I. Harris, *Int. J. Thermophys.* **20**:1587 (1999).
3. C. A. Benett, Jr. and R. R. Patty, *Appl. Opt.* **21**:49 (1982).
4. D. P. Almond, P. M. Patel, and H. Reiter, *Mater. Eval.* **45**:471 (1987).
5. S. K. Lau, D. P. Almond, and P. M. Patel, *J. Phys. D: Appl. Phys.* **24**:428 (1991).
6. J. D. Morris, D. P. Almond, P. M. Patel, and H. Reiter, *Photoacoustic and Photothermal Phenomena 2*, J. C. Murphy, J. W. Maclachlan Spicer, L. Aamodt, and B. S. H. Royce, eds. (Springer Verlag, Berlin, 1990), pp. 71–73.
7. A. C. Bento and D. P. Almond, *Meas. Sci. Technol.* **6**:1022 (1995).
8. R. E. Taylor, *Mater. Sci. Eng. A* **245**:160 (1998).
9. D. P. Almond, P. M. Patel, I. M. Pickup, and H. Reiter, *NDT Int.* **18**:17 (1985).
10. P. Cielo and S. Dallaire, *J. Mater. Eng.* **9**:71 (1987).
11. J. Morris, P. M. Patel, and H. Reiter, *Surf. Coat. Tech.* **34**:51 (1988).
12. A. S. Houlbert, P. Cielo, C. Moreau, and M. Lamontagne, *Int. J. Thermophys.* **15**:525 (1994).
13. B. K. Bein, J. Bolte, D. Dietzel, A. Haj Daoud, G. Kalus, F. Macedo, A. Linnenbrugger, H. Bosse, and J. Pelzl, *Surf. Coat. Tech.* **116–119**:147 (1999).
14. A. C. Bento, D. P. Almond, S. R. Brown, and I. G. Turner, *J. Appl. Phys.* **79**:6848 (1996).
15. L. Nicolaides and A. Mandelis, *J. Appl. Phys.* **90**:1255 (2001).
16. J. V. Beck and K. J. Arnold, *Parameter Estimation in Engineering and Science* (Wiley, New York, 1977), pp. 349–351.
17. J. V. Beck, B. Blackwell, and C. R. St. Clair, Jr., *Inverse Heat Conduction* (Wiley, New York, 1985), pp. 19–36.
18. A. Bendada and K.T. Nguyen, *Proc. Inverse Problems in Engineering: Theory and Practice,* Port Ludlow, June (ASME, New York, 1999), pp. 355–361.